Wang, Wei; Liu, Xuejun; Xu, Jin; Dore, Anthony J.; Xu, Wen. 2018. **Imbalanced nitrogen and phosphorus deposition in the urban and forest environments in southeast Tibet**.

# Imbalanced nitrogen and phosphorus deposition in the urban and forest environments in southeast Tibet

Wei Wang [1,2], Xuejun Liu [2], Jin Xu [1], Wen Xu [3,4*]

1. Xizang Agriculture and Animal Husbandry College, Nyingchi, Tibet, 860000, China

2. College of Resources and Environmental Sciences, China Agricultural University, Beijing 100193.

3. State Key Laboratory of Urban and Regional Ecology, Research Center for Eco-Environmental Sciences, Chinese Academy of Sciences, Beijing 100085, China

4. College of Resources and Environment, University of Chinese Academy of Sciences, Beijing 100049, China.

[*] Corresponding author (E-mail: hi.xuwen@163.com)

**Abstract**: In the last decades, in China a large amount of anthropogenic emissions has dramatically increased nitrogen (N) deposition and may lead to an imbalance of atmospheric N and phosphorus (P) inputs in terrestrial ecosystems. However, the status of N and P deposition in southeast Tibet is poorly understood. Here, we investigated spatial and monthly patterns of N and P deposition based on measurements of dissolved inorganic N (DIN, including ammonium N and nitrate N) and dissolved organic N (DON) and total dissolved P (TDP) in precipitation from March to October 2017 at an urban site in Nyingchi (NC) city and at a forest site in Sejila (SJL) Mountain. Over the study period, monthly total dissolved N (sum of DIN and DON) deposition fluxes summed 4.6 and 3.6 kg N $ha^{-1}$ at SJL and NC per year, respectively, of which dissolved organic nitrogen accounted for 35% and 38%. Monthly averages showed an increase trend from March to June, and then decrease in autumn months (September and October). At both two sites, ratios of ammonium to nitrate N in bulk deposition are greater than 1, indicating reduced N mainly from agricultural sources dominated N deposition in study area. Monthly TDP deposition fluxes summed to 0.68 and 0.58 kg P $ha^{-1}$ per year at SJL and NC, respectively, both of which showed an increased trend from March to May and decreased trend from July to October. The N/P ratio was 6.1 and 6.8 at NC and SJL, respectively.

Keyword: Nitrogen deposition; Phosphorus deposition; N/P ratio; Dissolved organic

nitrogen deposition; Tibet Plateau

## 1. Introduction

Nitrogen (N) and phosphorus (P) are essential elements for plant growth in terrestrial and marine ecosystems, but can also be considered as limiting elements when their supply does not meet demands by microbes and plants (Elser et al., 2007). Over the past few decades, reactive N (Nr) and P levels in the atmosphere have been increased significantly due to rapid development of industrialization and agricultural production, resulting in substantial increases in atmospheric N and P deposition to terrestrial ecosystems (Smil, 2000; Galloway et al., 2004; Liu et al., 2013). It has been estimated that at a global scale, anthropogenic Nr inputs to the biosphere were between 165–259 M ton N $yr^{-1}$ globally, N deposition fluxes were about 114 M ton N $yr^{-1}$ in the year 2000 and is expected to be a upward trend in the future (Peñuelas et al. 2012). In contrast, anthropogenic P inputs to biosphere were 22-26 M ton N $yr^{-1}$, and global P deposition were 3-4 M ton N $yr^{-1}$ since 1980 but had no obvious temporal trend (Peñuelas et al. 2013).

Due to the negative effects from excessive deposition on the environment, many studies have quantified magnitudes of N and/or P deposition at regional or national scales and differentiate their chemical compositions, especially N deposition (Lü et al., 2007; Duce et al., 2008; Jia et al., 2014; Lu et al., 2014; Zhu et al., 2015 Liang et al., 2016). For example, based on 5-year field measurements, Xu et al. (2015) reported that total N deposition (wet and dry) ranged from 2.9 kg N $ha^{-1}$ $yr^{-1}$to 83.8 kg N $ha^{-1}$ $yr^{-1}$ at 43 *in situ* monitoring sites across China. However, only few monitoring reports on atmosphere P deposition exist and are limited to particulate P (Luo et al., 2011; Parron et al., 2011; Hou et al., 2012; Du et al., 2016). It is well known that a complete quantification of P deposition is a big challenge, since P has no stable gaseous phase in the atmosphere and is mainly spread by wind in form of dust (Smil, 2000; Mahowald et al., 2008). At a national scale, Zhu at al. (2016) reported that wet P deposition ranged from 0.093 to 0.63 kg P $ha^{-1}$ $yr^{-1}$ at 41 *in situ* field stations across China. Their results also show that the ration of N to P in wet deposition was 77 (by

mass), much higher than N:P ratios (~47, based on molar) of global N deposition in continents and/ or those of terrestrial plants (22-30, based on molar) (Peñuelas et al., 2013).

The Qinghai-Tibet plateau, occupying about one-fourth of the land area of China (Zhang et al., 2002), is sensitive to global climate change (Liu et al., 2013; Xu et al., 2014). Long-term N addition can decrease the species richness of both vegetation and soil seed banks in alpine meadow ecosystems (Ma et al., 2014). At present, little is known about magnitude of N deposition in Qinghai-Tibet plateau (Liu et al., 2015; Zhu et al., 2015). In addition, atmospheric P deposition in the Qinghai-Tibet plateau remains unclear, especially in southeast Tibet, which accounted for 80% of the total forest area ($1.47\times10^7$ ha) in Tibet Province. In this paper, we presented estimates of bulk N and P deposition at two field monitoring sites in Nyingchi (NC) city and Sejila (SJL) mountain during the main rain season from March to October 2017, with the purposes being to quantify fluxes, forms and monthly variations of N and P deposition (as precipitation with continuously-open collector) to better understanding the current status of N and P deposition and impacts in remote region of China.

## 2. Materials and methods

### 2.1 Site description

For bulk N and P deposition measurements, the monitoring site in NC city was located at Xizang Agriculture and Animal Husbandry College (29°66'N 94°34'E 2990 m a.g.l.), southeast of the city, whereas that in SJL mountain was established at the National Field Scientific Observation Station of Alpine Forest Ecosystem (29°65'N 94°72'E 3950 m a.g.l.), on the edge of the NC city (**Fig. 1**). Nyingchi City is located beside the Niyang River, which was one of the main tributaries of the Brahmaputra. The climate is mainly dominated by warm air currents in the Indian Ocean, with an annual average temperature of 8.7℃ and an annual average precipitation of 650 mm. Tourism is a major local economic pillar industry. At NC site, there was no heavy industry nearby, and potential emission sources were a small village and agricultural fields. The SJL site was surrounded by original fir forest, in which undergrowth

vegetation were mainly *Sorbus*, *Rosa*, *Lonicera* and some other herbaceous plant. At this site, there were no anthropogenic Nr emission sources except for a state road (#318). Annual average temperature was -0.73℃ and annual average precipitation was about 1000 mm.

**2.2 Sampling and chemical analysis**

The rainwater samples were collected by continuously-open rain gauge, and thus contain mainly wet and unquantifiable fractions from gaseous and particulate Nr in dry-deposited process. In other word, wet deposition measured in the present work is actually bulk deposition. Rain gauge consists of a stainless steel funnel and glass bottle and was installed 1.2 m above the ground. After each precipitation event, the rainwater samples were thoroughly stirred and immediately stored in clean polyethylene bottles (50 ml), and then, the rainwater-collecting bottle was rinsed with deionized water to eliminate cross contamination. All samples were filtered with a 0.45 mm syringe filter (Tengda Inc., Tianjin, China), then filtrates were frozen in a refrigerator at -20 °C until prior to analysis in the laboratory.

The laboratory analysis was performed according to Chinese standard methods. Total dissolved nitrogen (TDN) was measured by alkaline potassium persulfate digestion-UV spectrophotometric method (GB11894-89); Nitrate nitrogen ($NO_3^-$-N) was measured by UV spectrophotometric Method; ammonium nitrogen ($NH_4^+$-N) was measured by reagent colorimetric method (GB7479-87)； Total dissolved phosphorus (TDP) was measured by ammonium molybdate spectrophotometric method (GB11893-89); Rainwater was digested using intelligent multiparameter digestion meter (LH-25A, Lianhua, China). $NO_3^-$-N, $NH_4^+$-N, and TDP were measured using ultraviolet and visible spectrophotometer (DR6000， HACH， America). DON concentration was defined as the difference between the TDN and inorganic N ($NH_4^+$-N and $NO_3^-$-N) concentrations (Zhang et al., 2012). During each analysis, rainwater samples were analyzed in duplicates and each analysis run consisted of 8 samples, one blank and a set of standard concentrations of $NH_4^+$-N, $NO_3^-$-N and TDN. Standard solutions were prepared in deionized water with concentrations ranges both 0-1 mg $L^{-1}$ for $NH_4^+$-N and $NO_3^-$-N, and 0-2 mg $L^{-1}$ for TDN. TDP contains phosphate

and dissolved organic P. Duplicate blank and standard reference materials (monopotassium phosphate, $KH_2PO_4$) methods were used for quality assurance.

### 2.3 Data calculation and analysis

Monthly Nr (TDN, $NH_4^+$-N, $NO_3^-$-N, DON) bulk deposition fluxes were calculated as follows:

$$N = \sum_{i=1}^{n} Ni * Pi / 100$$

Monthly dissolved phosphorus deposition fluxes were calculated as follows:

$$D = \sum_{i=1}^{n} Di * Pi / 100$$

where P is the precipitation per month(mm); N is bulk deposition fluxes of measured Nr species (TDN, $NH_4^+$-N, $NO_3^-$-N) (kg $ha^{-1}$ $month^{-1}$); D is the total dissolved phosphorus deposition fluxes (kg $ha^{-1}$ $month^{-1}$); *i* is the number of precipitations per month; *Pi* is the precipitation volume in *i* precipitation events; *Ni* is the volume-weighted mean concentration of measured Nr (TDN, $NH_4^+$-N, $NO_3^-$-N) components in *i* precipitation events; *Di* is the is the volume-weighted mean concentration of TDP in *i* precipitation events; 100 is the unit conversion factor of $mgm^{-2}$ to $kgha^{-1}$ .

### 2.4 Statistical analysis

Pearson correlation and regression analyses were conducted using the SPSS software package, version 20.0 (SPSS Inc., Chicago, IL), and significance was tested using a significance level (*P*) of 0.05.

### 2.5 Backward trajectory analysis

To recognize the potential sources and transport routes of air pollutants and precipitation clouds, air mass backward trajectory analysis was performed using the Hybrid-Single Particle Integrated Trajectory Model (HYSPLIT 4) (Xu et al., 2017), provided by the Air Resource Laboratory of National Oceanic and Atmospheric Administration (NOAA) (Stein et al., 2015; Roy et al., 2016). Meteorological data were input from the Global Data Assimilation System (GDAS) meteorological data archives of the Air Resource Laboratory, National Oceanic and Atmospheric Administration (NOAA). Three-day backward trajectories were calculated at 6 h

intervals (00:00, 06:00, 12:00, 18:00 UTC) on sampling days at both two study sites, with arrival height of 500 m above ground level. Then, cluster analysis was performed using the trajectories based on the total spatial variance (TSV) method (Draxler et al., 2012).

## 3. Results

### 3.1 Concentrations of Nr species and TDP in precipitation

Total rainfall amounts during March-October, the main rain season were 624.8 mm at NC and 838.3mm at SJL. Monthly precipitation amounts at SJL were higher than those at LZ city in all months except March and September (**Fig. 2a**). As showed in **Fig. 3**, total volume-weighted mean concentrations of $NH_4^+$-N were slightly higher than those of $NO_3^-$-N at both monitoring sites (0.19 versus 0.17 mg/L at SJL, and 0.22 versus 0.13 kg N $ha^{-1}$ at NC). In general, concentration of $NH_4^+$-N, DON, TDN and TDP at NC were all higher than those at SJL, but opposite behavior occurred for $NO_3^-$-N.

### 3.2 Atmosphere bulk deposition of Nr species and TDP

During the study period, monthly bulk deposition fluxes of $NO_3^-$-N, $NH_4^+$-N and DON were in the ranges of 0.01-0.23, 0.02-0.32, and 0.02-0.30 kg N $ha^{-1}$ at NC, respectively, whereas those were in the ranges of 0.02-0.35, 0.02-0.42, 0.02-0.47 kg N $ha^{-1}$ at SJL (**Figs. 2d-f**). At both two sites, bulk $NO_3^-$-N, $NH_4^+$-N and DON deposition fluxes generally show an increasing trend from March to June, and decrease trend from August to October. Compared with SJL, bulk deposition fluxes of $NO_3^-$-N at NC were lower in all months. Differently, bulk $NH_4^+$-N deposition fluxes were higher in March, May, September and October, bulk DON deposition fluxes were higher in July and September, but lower in other months. In total, bulk TDN deposition fluxes at NC were lower than those at SJL in all months except September (**Fig. 2b**). At each site, bulk TDN deposition fluxes showed a significant and positive correlation with precipitation amounts (**Fig. 4a**).

Monthly TDP deposition ranged from 0.01 to 0.16 kg $ha^{-1}$ at SJL, and from 0.01 to 0.14 kg P $ha^{-1}$at NC (**Fig. 2c**), with an increasing trend from March to May, and a

177 decreasing trend from Jul to October. The TDP deposition fluxes at SJL were higher
178 than those at NC in all months except April and September. A positive linear
179 relationship was found between TDP deposition fluxes and precipitation amounts at
180 both two sites (**Fig. 4b**).

181 Based on monthly averages in the main rainy season, bulk deposition fluxes of
182 TDN at SJL and NC summed 4.62 and 3.57 kg N $ha^{-1}$, respectively, with contributions
183 of 34% and 38% from DON. Bulk deposition fluxes of TDP summed 0.68 and 0.58 kg
184 P $ha^{-1}$ at SJL and NC, respectively. **(Fig. 5)**. The N/P ratio was 6.76 and 6.11 at SJL
185 and NC, respectively.

186 **4. Discussion**

187 A large variability in the monthly volume-weighted mean concentrations of Nr
188 species ($NH_4^+$-N, $NO_3^-$-N, and DON) and TDP in bulk precipitation was found at both
189 study sites. The lowest concentrations in bulk precipitation are associated with the
190 highest precipitation rates during summer months (Pineda Rojas and Venegas, 2010).
191 This can be explained because the first drops of rainfall perform an intense
192 atmospheric N and P scavenging, which increases the rainwater N and P concentration
193 in low rainfall events (Al-Khashman, 2009; Zhang et al., 2012; Sun et al., 2014). We
194 observed that $NH_4^+$-N and $NO_3^-$-N concentrations in bulk precipitation are positively
195 well correlated at the NC site ($R^2$=0.31, P<0.05) **(Fig. 6a)**, suggesting the existence of
196 dissolved $NH_4NO_3$ in precipitation from the atmosphere (Bertollini et al., 2016). The
197 presence of $NH_4NO_3$ in precipitation is related to volatilized fertilizers which have
198 been dissolved in rain droplets and deposited in rainfall events (Niu et al., 2014). The
199 relationships between DON and $NO_3^-$-N, and DON and $NH_4^+$-N concentrations at NC
200 were negative and statistically significant and were correlated by fitting a logarithmic
201 model (**Figs. 6b and c**). These results indicate similar origins of atmospheric organic
202 and inorganic N compounds in bulk deposition at NC sites. In contrast, the
203 correlations between $NH_4^+$-N, $NO_3^-$-N and DON were all not statistically significant
204 (P>0.05) at SJL. A non-significant correlation was also reported by several other
205 previous studies (Neff et al., 2002; Yang et al., 2010). The different chemical

composition correlations between the NC and SJL sites is likely linked with the differences in wet scavenging (in-cloud and below-cloud) of gases and particles and sources of DON, which can affect concentrations of inorganic and organic Nr species in precipitation (Seinfeld and Pandis, 1998; Yang et al., 2010).

Bulk N deposition is influenced by several factors, such as precipitation amounts and the seasonal variability of emission sources as well as N removal from the atmosphere via chemical and physical processes (Yu et al., 2011; Kuang et al., 2016; Liu et al., 2016; Calvo-Fernández et al., 2017; Xing et al., 2017; Xu et al., 2018). The present results show that precipitation amounts varies greatly between different months at the two study sites, with higher levels in May, June, July, and August **(Fig. 2a)**. Higher bulk N and TDP deposition fluxes were also found corresponding to those months **(Fig. 2b,c)**. We also observed relatively high $NO_3^-$-N deposition fluxes in June and September at SJL. Not surprisingly, a high deposition level was observed in September when precipitation amounts were relatively small. Diesel generators, a major $NO_x$ emission source (Liu et al., 2011), were frequently used for construction and reconstruction works carrying out only in September at SJL. Thus, an elevated atmospheric $NO_x$ level resulting from large amounts of $NO_x$ emissions from Diesel generators is a likely explanation for high $NO_3^-$-N deposition fluxes. Estimated $NH_4^+$-N deposition fluxes were higher in May at NC, which is likely due to the increased volatilization of $NH_3$ from local agricultural activities (cultivation and fertilization) in April and May caused by higher temperatures (Xu et al., 2014).

DON categories mainly include reduced organic nitrogen, oxidized organic nitrogen and biological organic nitrogen (Graedel et al., 1986). It has been reported that the averaged DON deposition flux was 6.84 kg N $ha^{-1}$ $yr^{-1}$, and accounted for more than 50% of total N deposition fluxes in a forest ecosystem (Zhang et al., 2012). A similar phenomenon was also observed in the present work. DON deposition fluxes were extremely high in June at SJL, mainly due to relatively high pollen grain sedimentation in summer (Bovallius et al., 1978). Similarly monthly TDP deposition fluxes were higher during May-July compared to other months at both monitoring site, especially at SJL (**Fig. 4**). This can be attributed to the fact that atmosphere

pollen grain sedimentation is the major source of atmospheric P deposition (Mahowald et al. 2008). It has been estimated that the phosphorus content was about 0.5% in *Euphoria longan* pollen grain (Liu et al., 1995). SJL Mountain, the selected monitoring site was located in a clearing surrounded by plants like *Abies georgei*, *Sorbus rehderiana*, *Rosa multiflora*, all of which flowered during May-late July every year, thus lead to relatively higher bulk TDP deposition.

For the Qinghai-Tibet plateau, bulk N deposition fluxes averaged 7.62 ± 8.60 kg N $ha^{-1}$ $yr^{-1}$ at two urban and forest sites (Xu et al., 2015)**Error! Bookmark not defined.**. Wet N deposition levels ranged from 0.44 to 1.55 kg N $ha^{-1}$ $yr^{-1}$ for inorganic N at 5 remote sites (Liu et al., 2015), with 8.36 ± 4.19 kg N $ha^{-1}$ $yr^{-1}$ estimated for total dissolved N deposition at a regional scale (Zhu et al., 2016). These results imply the existence of large spatial variability in wet/bulk N deposition in the Tibet plateau. By contrast, bulk TDN deposition fluxes we measured were 4.62 and 3.57 kg N $ha^{-1}$ at SJL and NC, respectively. According to the China Meteorological Data Network statistics (http://data.cma.cn/data/weatherBk.html), the average precipitation amount from November to February was 11.4mm during the last 30 years (1981-2010) next year in NC city, accounting for 1.6% of the annual precipitation amount. Given such relatively low precipitation from October to February, the fluxes measured during March-October at NC and SJC can reflect their respective annual deposition levels to some extent. Similar research hasreported that average total dissolved N deposition was 7.9 kg N $ha^{-1}$ $yr^{-1}$ during 2012-2013 in a southeast forest ecosystem (Liu et al., 2016). It is commonly accepted that N and P deposition have been enhanced by human activities (Peñuelas et al. 2012; Peñuelas et al., 2013). However, bulk N deposition fluxes were higher at SJL compared with those at NC **(Fig. 5),** although the former is considered to be a remote forest monitoring site. This is mainly due to higher precipitation amounts at SJL than at NC **(Fig. 2a)**, since bulk N deposition fluxes were influenced not only by rainfall Nr concentration but also by precipitation amounts (Xu et al., 2015) Compared with other Nr species, bulk $NO_3^-$-N deposition fluxes differed clearly between SJL and NC **(Fig. 3)**. One explanation is that SJL mountain monitoring site is located near State Road

(#318) (which is a major road in Tibet), and thus was polluted by $NO_x$ emissions from fossil fuel combustion in transportation (Liu et al. 2011). It should be pointed out that bulk deposition is used here to refer to wet plus part of the dry deposition collected by rain gauges that remain open to the atmosphere. Based on a full two-year (2014-2015) measurements of monthly $NO_2$ and $NH_3$ concentration at a suburban site in Xining City, Qinghai Province, Xu et al. (2017b) found that dry N deposition accounted for 46% of the total deposited N. This highlights the importance of dry deposition in the urban environment, even in remote area of China. Thus, to assess the influence from dry deposition, a comparison of mean bulk deposition and wet-only deposition at two study sites is recommended in future studies.

The $NH_4^+$-N and $NO_3^-$-N concentrations in precipitation reflect the composition of gaseous and particulate Nr species in the atmosphere (Celle-Jeanton et al., 2009; Niu et al., 2014). Thus, the $NH_4^+$-N/$NO_3^-$-N ratio in precipitation is a useful tool to identify the predominant sources of N depositions in a targeted area (Xu et al., 2015). It is widely agreed that a $NH_4^+$-N/$NO_3^-$-N deposition ratio <1 within industrialized regions and >1 within intensive agricultural regions (Xu et al., 2009). In the present study, $NH_4^+$-N/$NO_3^-$-N ratios in bulk deposition are greater than 1 at both the NC site (average 1.70) and the SJL site (average 1.14), indicating that agricultural sources (e.g., fertilized pastureland and farmland areas) dominate atmospheric N deposition in the target area relative to industrial sources (e.g., transportation and combustion) . In addition to local emission sources, long-range atmospheric transport of air mass also has influences on N and/or P deposition at remote areas in Tibet (Liu et al., 2015; Xu et al., 2017a). Based on the origin areas and transport directions, three and four categories of air masses were identified from the entire set of trajectories at the NC and SJL sites, respectively (**Fig. 7**). It is evident that the precipitation events during the sampling period at both sites were dominated by air masses from the south region, with the proportion of 65% and 62%, respectively. This is becausesoutheast Tibet is influenced by a southwest monsoon and the wind is mainly from the south (Yang et al., 2012) where no heavy pollution sources are located. In addition, the volume-weighted mean concentrations of DIN ($NH_4^+$-N and $NO_3^-$-N), DON and TDP

296 in precipitation associated with two categories air masses (south and northwest) were
297 analyzed. As presented in Table 1, there were no large differences in concentrations
298 between the two directions. These results together to some extent suggest that
299 regional transport has little influences on N and P deposition at the two study sites,
300 which is more likely to be driven by local emission sources.

301 The chemical form of N input from the atmosphere plays a vital role in
302 regulating nutrient assimilation processes for plant growth in a wide variety of
303 ecosystems (Stevens et al., 2011; Harmens et al., 2014; Izquieta-Rojano et al., 2016).
304 Sheppard et al. (2014) demonstrated that $NH_4^+$-N is more likely to be toxic to plant
305 root assimilation compared to $NO_3^-$-N. We found that $NH_4^+$-N input was higher than
306 $NO_3^-$-N input, which might have potential harmful effects on local vegetation. Besides,
307 $NH_4^+$-N deposition has a greater influence on vegetation composition compared to
308 $NO_3^-$-N deposition (van den Berg et al., 2016), since $NH_4^+$-N deposition can lead to
309 soil acidification by release of $H^+$ ions (Du et al., 2015); being the main pathway of
310 biodiversity loss in ecosystems adapted to N-poor conditions (Boutin et al., 2015).
311 This could greatly affect biodiversity in subalpine coniferous forest and temperate
312 deciduous conifer mixed forest in southeast Tibet, which is recognized as a
313 biodiversity hotspot and is sensitive to elevated N deposition (You et al., 2013; Zhang
314 et al., 2014). Regarding the seasonal variation in bulk precipitation, the high $NH_4^+$-N
315 and $NO_3^-$-N deposition fluxes in summer (June, July and August) could affect the
316 nutrient balance of N-poor ecosystems such as native fir forest (Edfast et al. 1990),
317 since this period is the vegetation growing season and deposited N can be absorbed by
318 vegetation in maximum degree. Earlier studies have demonstrated that an increase in
319 N deposition could result in a series of adverse effects on forest ecosystems, including
320 soil acidification (Bergkvist et al., 1992), ion leaching (Foster et al. 1989), increase of
321 leaf N concentration and photosynthetic rate (Magill et al. 2000; Nakji at al., 2001).

322 Atmospheric wet P deposition was on average 0.21 kg P $ha^{-1}$ $yr^{-1}$ (ranging from
323 0.002 to 2.53 kg P $ha^{-1}$ $yr^{-1}$) at 41 in situ observation sites across China and was 0.21
324 kg P $ha^{-1}$ $yr^{-1}$on a global scale (Zhu et al., 2016; Tipping et al., 2014). At a point scale,
325 earlier studies based on field measurements demonstrated that bulk P deposition was

326 1.82 kg P $ha^{-1}yr^{-1}$ in Nanjing city (Sun et al., 2014), and wet P deposition was 0.9 kg P
327 $ha^{-1}yr^{-1}$ in Lake Taihu (Yang et al 2007). In the present study, bulk P deposition fluxes
328 were 0.58 and 0.68 kg P $ha^{-1}$ at the NC and SJL sites, respectively. Obviously,
329 estimated bulk P deposition in the study area was higher than the average levels in
330 China and in the world, but lower than those measured in southeast China.

331 Unbalanced human-induced N and P inputs to the atmosphere led to an increase
332 in the N/P ratio in wet/bulk deposition. Many studies has illustrated that the current
333 situation of N and P deposition shifts all over the world (Peñuelas et al. 2013;
334 Peñuelas et al., 2015). For example, foliar N concentrations from non-agricultural
335 ecosystems throughout China significantly increased from 1980 to 2000 in the context
336 of enhanced N deposition (Liu et al., 2013). It has been estimated that the N/P ratio in
337 bulk deposition was about 21.2 at a global scale and about 77 (based on mass) at a
338 national scale in China. At a regional scale, N/P ratios (based on mass) varied greatly
339 in different regions of China. For example, the N/P ratio was 10 in Yangzonghai (Yu
340 et al., 2017), 77 in Hangjiahu area (Wang et al., 2015), 30 in Nanjing city (Sun et al.,
341 2014), 14 in Taihu lake (Yang et al., 2007). Furthermore, due to enhanced N
342 deposition globally and intensified human activities in Tibet, Nr deposition is
343 expected to increase continuously in the future, which could promote plant growth
344 and further affect local plant community structure or phytocoenosis evolution.

345 **5. Conclusions**

346 The present study measured bulk deposition fluxes of DIN, DON and TDP at an
347 urban (NC) site and a forest (SJL) site in the southeast of the Tibetan Plateau during
348 the i main rainy seasons from March to October 2017. Total deposition of TDN and
349 TDP was 4.62 kg N $ha^{-1}$ $yr^{-1}$ and 0.68 kg P $ha^{-1}$ $yr^{-1}$ at SJL, and 3.57 kg N $ha^{-1}$ $yr^{-1}$ and
350 0.58 kg P $ha^{-1}$ $yr^{-1}$ at NC, respectively, with N/P ratios of 6.8 and 6.1. TDN and TDP
351 deposition fluxes were higher at SJL compared with those at NC, but the opposite
352 phenomenon was observed for TDN and TDP concentrations. At both o sites, DIN
353 deposition accounted for 65% and 62% of TIN deposition fluxes, with
354 $NH_4^+$-N/$NO_3^-$-N ratios greater than 1. In order to obtain systematic knowledge on the

sources, composition and rates of N and P deposition as well as its ecological effects, additional monitoring sites, covering typical land use types in the region, should be established in the futureadopting standardized sampling protocols and analytical methods.

**Acknowledgements**

This work was supported by Tibet Youth Science Foundation (2016ZR-NQ-09), the National Key R&D Program of China (2017YFC0210106), and the National Natural Science Foundation of China (41705130). The authors thank all members of the National Field Scientific Observation Station of Alpine Forest Ecosystem for their co-operation during this experiment.

## References


Al-Khashman, O.A., 2009. Chemical characteristics of rainwater collected at a western site of Jordan. Atmos. Res. 91, 53–61.

Bergkvist, B. O., Folkeson, L., 1992. Soil acidification and element fluxes of a Fagus-sylvatica, forest as influenced by simulated nitrogen deposition. Water Air Soil Poll. 65(1–2), 111–133.

Bertollini, T., Flechard, C.R., Fattore, F., Nicolini, G., Stefani, P., Materia, S., Valentini, R., Laurin, G.V., Castaldi, S., 2016. DRY and BULK atmospheric nitrogen deposition to a West-African humid forest exposed to terrestrial and oceanic sources. Agric. For. Meteorol. 218–219, 184–195.

Boutin, M., Lamaze, T., Couvidat, F., Pornon, A., 2015. Subalpine Pyrenees received higher nitrogen deposition than predicted by EMEP and CHIMERE chemistry-transport models. Sci. Rep. 5, 12942.

Bovallius, A., Bucht, B., Roffey, R., Anäs, P., 1978. Three-year investigation of the natural airborne bacterial flora at four localities in Sweden. Appl. Environ. Microb. 35(5), 847–52.

Calvo-Fernández, J., Marcos, E., Calvo, L., 2017. Bulk deposition of atmospheric inorganic nitrogen in mountainous heathland ecosystems in north-western Spain. Atmos. Res. 183, 237–244.

Celle-Jeanton, H., Travi, Y., Löye-Pilot, M.D., Huneau, F., Bertrand, G., 2009. Rainwater chemistry at a Mediterranean inland station (Avignon, France): local contribution versus long-range supply. Atmos. Res. 91, 118–126.

Draxler, R., Stunder, B., Rolph, G., Stein, A., Taylor, A., 2012. HYSPLIT4 user’s guide, version 4, report, NOAA, Silver Spring, MD.

Du, E., De Vries, W., Liu, X., Fang, J., Galloway, J.N., Jiang, Y., 2015. Spatial boundary of urban 'acid islands' in southern China. Sci. Rep. 5:12625

Du, E.Z., De Vries, W., Han, W.X., Liu, X.J., Yan, Z.B., Jiang, Y., 2016. Imbalanced phosphorus and nitrogen deposition in china's forests. Atmos. Chem. Phys. 16(13), 8571-8579.

Duce, R.A., Laroche, J., Altieri, K., Arrigo, K.R., Baker, A.R., Capone, D.G., Cornell, S., Dentener, F., Galloway, J., Ganeshram, R.S., Geider, R. J., Jickells, T., Kuypers, M.M., Langlois, R., Liss, P.S., Liu, S.M., Middelburg, J.J., Moore, C.M., Nickovic, S., Oschlies, A., Pedersen, T., Prospero, J., Schlitzer, R., Seitzinger, S., Sorensen, L.L., Uematsu, M., Ulloa, O., Voss, M., Ward, B., Zamora, L.2008. Impacts of atmospheric anthropogenic nitrogen on the open ocean. Science 320(5878), 893-897.

Edfast, A.B., Näsholm, T., Ericsson, A., 1990. Free amino acid concentrations in needles of Norway spruce and scots pine trees on different sites in areas with two levels of nitrogen deposition. Can. J. Forest Res. 20(8), 1132-1136.

Elser, J.J., Bracken, M.E.S., Cleland, E.E., Gruner, D.S., Harpole, W.S., Hillebrand, H., Ngai, J.T., Seabloom, E.W., Shurin, J.B., Smith, J.E., 2007, Global analysis of nitrogen and phosphorus limitation of primary producers in freshwater, marine and terrestrial ecosystems, Ecol. Lett.10(12), 1135–1142,

Foster, N.W., Hazlett, P.W., Nicolson, J.A., Morrison, I.K., 1989. Ion leaching from a sugar maple forest in response to acidic deposition and nitrification. Water Air Soil Poll. 48(1-2), 251-261.

Galloway, J.N., Dentener, F.J., Capone, D.G., Boyer, E.W., Howarth, R.W., Seitzinger, S.P., Asner, G.P., Cleveland, C.C., Green, P.A., Holland, E.A., Karl, D.M., Michaels, A.F., Porter, J.H., Townsend, A.R., Vorosmarty, C.J., 2004. Nitrogen cycles: past, present, and future. Biogeochemistry 70, 153-226.

Graedel, T.E., Hawkins, D.T., Claxton, L. D., 1986. Atmospheric Chemical Compounds [M]. Atmospheric Chemical Compounds, 68(49):579–651.

Harmens, H., Schnyder, E., Thöni, L., Cooper, D.M., Mills, G., Leblond, S., Mohr, K., Poikolainen, J., Santamaría, J., Skudnik, M., Zechmeister, H.G., Lindroos, A.J., HanusIllnar, A., 2014. Relationship between site-specific nitrogen concentrations in mosses and measured wet bulk atmospheric nitrogen deposition across Europe. Environ. Pollut. 194, 50–59.

Hou, P.Q., Ren, Y.F., Zhang, Q.Q., Lu, F., Ouyang, Z.Y., Wang, X.K., 2012. Nitrogen and phosphorous in atmospheric deposition and roof runoff. Pol. J Environ. Stud.

21(6), 1621-1627.

Izquieta-Rojano, S., García-Gómez, H., Aguillaume, L., Santamaría, J.M., Tang, Y.S., Santamaría, C., Valiño, F., Lasheras, E., Alonso, R., Àvila, A., Cape, J.N., Elustondo, D., 2016. Throughfall and bulk deposition of dissolved organic nitrogen to holm oak forests in the Iberian Peninsula: flux estimation and identification of potential sources. Environ. Pollut. 210, 104–112.

Jia, Y.L., Yu, G.R., He, N.P., Zhan, X.Y., Fang, H.J., Sheng, W.P., Yao Z., Zhang D.Y., Wang Q.F., 2014. Spatial and decadal variations in inorganic nitrogen wet deposition in china induced by human activity. Sci. Rep. 4(4), 3763.

Kuang, F.H., Liu, X.J., Zhu, B., Shen, J.L., Pan, Y.P., Su, M.M., Goulding K., 2016. Wet and dry nitrogen deposition in the central Sichuan basin of china. Atmos. Environ.143, 39-50.

Liang, T., Tong, Y.A., Liu, X.J., Xu, W., Luo, X.S., Christie, P., 2016. High nitrogen deposition in an agricultural ecosystem of Shanxi, china. Environ. Sci. Pollut. R. 23(13), 13210-13221.

Liu, J.Q., Zhang, Q.Q., Wu, W.S., Lin, W.Q., 1995. Analysis of pollen nutrition components of *Dimocarpus* longan, Territ. Nat. Resour. Stud. 3, 73-73. (In Chinese)

Liu, X.J., Duan, L., Mo, J.M., Du, E.Z., Shen, J.L., Lu, X.K., Zhang, Y., Zhou, X.B., He, C.N., Zhang, F.S., 2011. Nitrogen deposition and its ecological impact in china: an overview. Environ. Pollut. 159(10), 2251.

Liu, X.J., Zhang, Y., Han, W.X., Tang, A.H., Shen, J.L., Cui, Z.L., Vitousek, P., Erisman, J.W., Goulding, K., Christie, P., Fangmeier, A., Zhang, F.S., 2013. Enhanced nitrogen deposition over China. Nature 494, 459-462.

Liu, Y.W., Xu-Ri, Xu, X.L., Wei, D., Wang, Y.H., Wang, Y.S., 2013. Plant and soil responses of an alpine steppe on the Tibetan Plateau to multi-level nitrogen addition. Plant Soil, 373, 515– 529.

Liu, Y.W., Xu-Ri, Wang, Y.S., Pan, Y.P., Piao, S.L., 2015. Wet deposition of atmospheric inorganic nitrogen at five remote sites in the Tibetan plateau. Atmos. Chem. Phys. 15(20), 11683-11700.

Liu, Z.Y., Zhou, Y.J., Li, H., Han L. 2016. Variation Features of nitrogen deposition fluxes in forest throughfall and its influencing factors in southeastern Tibet. Meteor. Sci. Tech. 44 (10), 834-840. (In Chinese with English abstract)

Lü, C.Q., Tian, H.Q., 2007. Spatial and temporal patterns of nitrogen deposition in china: synthesis of observational data. J Geophys. Res-Atmos. 112(D22), 229-238.

Lü, C.Q., Tian, H.Q., 2014. Half-century nitrogen deposition increase across china: a gridded time-series data set for regional environmental assessments. Atmos. Environ. 97, 68-74.

Luo, J., Wang, X.R., Yang, H., Yu, J.Z., Yang, L.Y., Qin, B.Q., 2011. Atmospheric phosphorus in the northern part of Lake Taihu, china. Chemosphere 84(6), 785-791.

Ma, Z., Ma, M.J., Baskin, J.M., Baskin, C.C., Li, J.Y., Du, G.Z., 2014. Responses of alpine meadow seed bank and vegetation to nine consecutive years of soil fertilization. Ecol. Eng. 70(9), 92-101.

Magill, A.H., Aber, J.D., Berntson, G.M., Mcdowell, W.H., Nadelhoffer, K.J., Melillo, J.M., 2000. Long-term nitrogen additions and nitrogen saturation in two temperate forests. Ecosystems 3(3), 238-253.

Mahowald, N., Jickells, T.D., Baker, A.R., Artaxo, P., Benitez-Nelson, C.R., Bergametti, G., Bond T.C., Chen Y., Cohen, D.D., Herut, B., Kubilay, N., Losno, R., Luo, C., Maenhaut, W., McGee, K.A., Okin, G.S., Siefert, R.L., Tsukuda, S., 2008. Global distribution of atmospheric phosphorus sources, concentrations and deposition rates, and anthropogenic impacts. Global Biogeochem. Cy. 22(4), 37-42.

Nakji, T., Fukami, M., Dokiya, Y., Izuta, T., 2001. Effects of high nitrogen load on growth, photosynthesis and nutrient status of *cryptomeria japonica* and *pinus densiflora* seedlings. Trees-Struct Funct. 15(8), 453–461.

Neff, J.C, Holland, E.A, Dentener, F.J, McDowell, W.H, Russell, K.M., 2002. The origin, composition and rates of organic nitrogen deposition: A missing piece of the nitrogen cycle? Biogeochemistry 57–58, 99–136.

503 Niu, H.W., He, Y.Q., Lu, X.X., Shen, J., Du, J.K., Zhang, T., Pu, T., Xin, H.J., Chang,
504 L., 2014. Chemical composition of rainwater in the Yulong Snow Mountain
505 region, southwestern China. Atmos. Res. 144, 195–206.
506 Parron, L.M., Bustamante, M.M.C., Markewitz, D., 2011. Fluxes of nitrogen and
507 phosphorus in a gallery forest in the Cerrado of central Brazil. Biogeochemistry
508 105(1–3), 89–104.
509 Peñuelas, J., Poulter, B., Sardans, J., Ciais, P., van der Velde, M., Bopp, L., Boucher,
510 O., Godderis, Y., Hinsinger, P. Llusia, J., Nardin, E., Vicca, S., Obersteiner, M.,
511 Janssens, I.A. 2013. Human-induced nitrogen–phosphorus imbalances alter
512 natural and managed ecosystems across the globe. Nat Commun. 4(1), 2934.
513 Peñuelas, J., Sardans, J., Rivas-Ubach, A., Janssens, I. A, 2012. The human‐induced
514 imbalance between C, N and P in earth's life system. Global Change Biol. 18(1),
515 3–6.
516 Pineda Rojas, A.L., Venegas, L.E., 2010. Inter annual variability of estimated monthly
517 nitrogen deposition to coastal waters due to variations of atmospheric variables
518 model input. Atmos. Res. 96, 88–102.
519 Roy, A., Chatterjee, A., Tiwari, S., Sarkar, C., Das, S.K., Ghosh, S.K., Raha, S., 2016.
520 Precipitation chemistry over urban, rural and high altitude Himalayan stations in
521 eastern India. Atmos. Res. 181, 44–53.
522 Seinfeld J, Pandis S. Atmospheric Chemistry and Physics. New York: Wiley; 1998.
523 Smil, V., 2000, Phosphorus in the environment: Natural flows and human
524 interferences. Annu. Rev. Energy Environ. 25, 53–88.
525 Sheppard, L.J., Leith, I.D., Mizunuma, T., Leeson, S., Kivimaki, S., Cape, J.N., van
526 Dijk, N., Leaver, D., Sutton, M.A., Fowler, D., Van den Berg, L.J.L., Crossley, A.,
527 Field, C., Smart, S., 2014. Inertia in an ombrotrophic bog ecosystem in response
528 to 9 years' realistic perturbation by wet deposition of nitrogen, separated by form.
529 Glob. Chang. Biol. 20, 566–580.Stein, A.F., Draxler, R.R., Rolph, G.D., Stunder,
530 B.J.B., Cohen, M.D., Ngan, F., 2015. NOAA's HYSPLIT atmospheric transport
531 and dispersion modeling system. Bull. Am. Meteorol. Soc. 96 (12), 2059–2077
532 Stevens, C.J., Manning, P., Van den Berg, L.J.L., De Graaf, M.C.C., Wamelink,

G.W.W., Boxman, A.W., Bleeker, A., Vergeer, P., Arroniz-Crespo, M., Limpens, J., Lamers, L.P.M., Bobbink, R., Dorland, E., 2011. Ecosystem responses to reduced and oxidized nitrogen inputs in European terrestrial habitats. Environ. Pollut. 159, 665–676.

Sun, L.Y, Liu, Y.L, Wang, J.Y, Khalil, M.A.K, Zou, J.W, Xiong, Z.Q., 2014. Atmospheric nitrogen and phosphorus deposition at three sites in Nanjing, China, and possible links to nitrogen deposition sources. Clean-Soil Air Water 42 (11), 1–10.

Tipping, E., Benham, S., Boyle, J.F., Crow, P., Davies, J., Fischer, U., Guyatt, H., Helliwell, R., Jacksonblake, L., Lawlor, A.J., Monteith, D.T., Rowe, E.C., Toberman, H., 2014. Atmospheric deposition of phosphorus to land and freshwater. Environ. Sci. Proc. Impacts 16(7), 1608-1617.

Van den Berg, L.J.L., Jones, L., Sheppard, L.J., Smart, S.M., Bobbink, R., Dise, N.B., Ashmore, M.R., 2016. Evidence for differential effects of reduced and oxidized nitrogen deposition on vegetation independent of nitrogen load. Environ. Pollut. 208, 890–897.

Xing, J.W., Song, J.M., Yuan, H.M., Li, X.G., Li, N., Duan, L.Q., Kang, X.M., Wang, Q.D., 2017. Fluxes, seasonal patterns and sources of various nutrient species (nitrogen, phosphorus and silicon) in atmospheric wet deposition and their ecological effects on Jiaozuo bay, north china. Sci Total Environ. 576(576), 617.

Xu, W., Zheng, K., Liu, X.J., Meng, L.M., Huaitalla, R.M., Shen, J.L., Hartung E., Gallmann, E., Roelcke, M., Zhang F.S., 2014. Atmospheric $NH_3$ dynamics at a typical pig farm in china and their implications. Atmos. Pollut. Res. 5(3), 455-463.

Xu, W., Luo, X.S., Pan, Y.P., Zhang, L., Tang, A.H., Shen, J.L., Zhang, Y., Li, K.H., Wu, Q.H., Yang, D.W., Zhang, Y.Y., Xue, J., Li, W.Q., Li, Q.Q., Tang, L., Lu, S.H., Liang, T., Tong, Y.A., Liu, P., Zhang, Q., Xiong, Z.Q., Shi, X.J., Wu, L.H., Shi, W.Q., Tian, K., Zhong, X.H., Shi, K., Tang, Q.Y., Zhang, L.J., Huang, J.L., He, C.E., Kuang, F.H., Zhu, B., Liu, H., Jin, X., Xin, Y.J., Shi, X.K., Du, E.Z., Dore, A.J., Tang, S., Collett, J.L., Goulding, K., Sun, Y.X., Ren, J., Zhang, F. S.,

563 Liu, X. J., 2015. Quantifying atmospheric nitrogen deposition through a
564 nationwide monitoring network across china. Atmos. Chem. Phys. 15(21),
565 18365-18405.
566 Xu, W., Song, W., Zhang, Y.Y., Liu, X.J., Zhang, L., Zhao, Y.H., Liu, D.Y., Tang, A.H.,
567 Yang, D.W., Wang, D.D., Wen, Z., Pan, Y.P., Fowler, D., Collett Jr, J.L., Erisman,
568 J.W., Goulding, K., Li, Y., Zhang, F.S., 2017. Air quality improvement in a
569 megacity: implications from 2015 Beijing Parade Blue pollution control actions.
570 Atmos. Chem. Phys. 17 (1), 31-46.
571 Xu, W., Jin, X., Luo, X.H., Feng, Z.Z., Zhang, L., Pan, Y. P., Liu, X. J., 2017b. Dry
572 and bulk nitrogen deposition in suburbs of Xining City. Environ. Sci. 38(4),
573 1279-1288.
574 Xu, W., Zhao, Y.H., Liu, X.J., Dore, A.J., Zhang, L., Liu, L., Cheng, M.M., 2018.
575 Atmospheric nitrogen deposition in the Yangtze River basin: Spatial pattern and
576 source attribution. Environ. Pollut. 232, 546-555.
577 Xu, Z., Yan, X., Xiong, Z., Xie, Y., Xing, G., Shi, S., Zhu, Z., 2009. Spatial and
578 temporal variation of inorganic nitrogen wet deposition to the Yangtze River
579 delta region, china. Water Air Soil Poll. 203(1-4), 277-289.
580 Yang, L., Qin, B., Hu, W., Luo, L., Song, Y., 2007. The atmospheric deposition of
581 nitrogen and phosphorus nutrients in Taihu Lake. Oceanologia Etlimnologia
582 Sinica. 38(2):104-110. (In Chinese with English abstract).
583 Yang, R., Hayashi, K., Zhu, B., Li, F.Y., Yan, X.Y., 2010. Atmospheric $NH_3$ and $NO_2$
584 concentration and nitrogen deposition in an agricultural catchment of Eastern
585 China. Sci. Total Environ. 408, 4624-4632.
586 Yang X X, Xu B Q, Yang W, Qu D M., 2012. The Indian monsoonal influence on
587 altitude effect of $\delta^{18}O$ in surface water on southeast Tibetan Plateau. Sci
588 China Earth Sci, 55: 438–445.
589 You J., Feng J., 2013. Plant biodiversity and flora composition in Southeast Tibet.
590 Ecol. Environ. Sci. 22(2): 207-212. (In Chinese with English abstract).
591 Yu G.Y., Yang C.L., Yang C.L., Liu K., Yang H.Y., Zhang J.L.,2017. Atmospheric
592 deposition of nitrogen and phosphorous in Lake Yangzonghai, Yunnan Province.

593 J Lake Sci. 2017, 29(5):1134-1142. (In Chinese with English abstract)
594 Yu, W.T., Jiang, C.M., Ma, Q., Xu, Y.G., Zou, H., Zhang, S.C., 2011. Observation of
595 the nitrogen deposition in the lower liaohe river plain, northeast china and
596 assessing its ecological risk. Atmos. Res. 101(1), 460-468.
597 Zhang, Y. L., Li, B. Y., Zheng, D., 2002. A discussion on the boundary and area of the
598 Tibetan Plateau in China. Geographical Res., 21(1), 1–8, (in Chinese with
599 English abstract).
600 Zhang, Y., Song, L., Liu, X.J., Li, W.Q., Lü, S.H., Zheng, L.X., Bai, Z.C., Cai, G.Y.,
601 Zhang, F.S., 2012. Atmospheric organic nitrogen deposition in China. Atmos.
602 Environ. 46, 195–204.
603 Zhang, Y.H., Lu, X.T., Isbell, F., Stevens, C., Han, X., He, N.P, Zhang, G.M., Yu, Q.,
604 Huang, J.H., Han, X.G., 2014, Rapid plant species loss at high rates and at low
605 frequency of N addition in temperate steppe. Global Change Boil. 20(11):
606 3520-3529.
607 Zhu, J.X., He, N.P., Wang, Q.F., Yuan, G.F., Wen, D., Yu, G.R., Jia, Y.L., 2015. The
608 composition, spatial patterns, and influencing factors of atmospheric wet
609 nitrogen deposition in Chinese terrestrial ecosystems. Sci. Total Environ.
610 511(511), 777-785.
611 Zhu, J.X., Wang, Q.F., He, N.P., Smith, M.D., Elser, J.J., Du, J.Q., Yuan, G.F., Yu G.R.,
612 Yu, Q., 2016. Imbalanced atmospheric nitrogen and phosphorus depositions in
613 china: implications for nutrient limitation. J.Geophys. Res-Biogeo. 121(6):1-12.
614 GB 11894-89, Water quality-Determination of total nitrogen-Alkaline potassium
615 persulfate digestion-UV spectrophotometric method. China national bureau of
616 technical supervision, 1989 (in Chinese).
617 GB 7479-87, Water quality-Determination of ammonia nitrogen-Nessler’s reagent
618 spectrophotometry. China national bureau of technical supervision, 1987 (in
619 Chinese).
620 GB 11893-89, Water quality-Determination of total phosphorus-Ammonium
621 molybdate spectrophotometric. China national bureau of technical supervision,
622 1989 (in Chinese).

623

624 **Figure captions**

625 Figure 1. Location of the two monitoring sites in Nyingchi city, southeast Tibet

626 Figure 2. Monthly precipitations and bulk deposition fluxes of N and P at the two
627 monitoring sites

628 Figure 3. Volume-weighted mean concentration of Nr species and P in precipitation

629 Figure 4. Correlations between precipitation and N deposition fluxes (a) and P
630 deposition fluxes (b) at the two sampling sites

631 Figure 5. Total N and P deposition fluxes during the observation period at the two
632 monitoring sites

633 Figure 6. Correlation between concentrations of $NO_3^-$-N and $NH_4^+$-N (a), between
634 concentrations of $NO_3^-$-N and DON (b) and concentrations of $NH_4^+$-N and DON (c) at
635 the two sites

636 Figure 7. 3-day backward trajectories at NC (a) and SJL (b) sites in southeast Tibet.
637 Lines with different colors show the clustering trajectories.

638

**Figure 1**

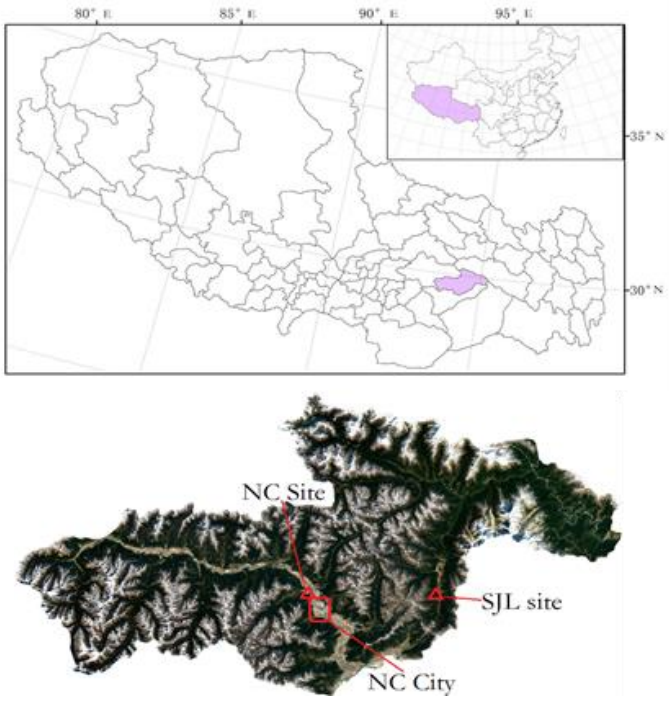

649

650 **Figure2**

651

652

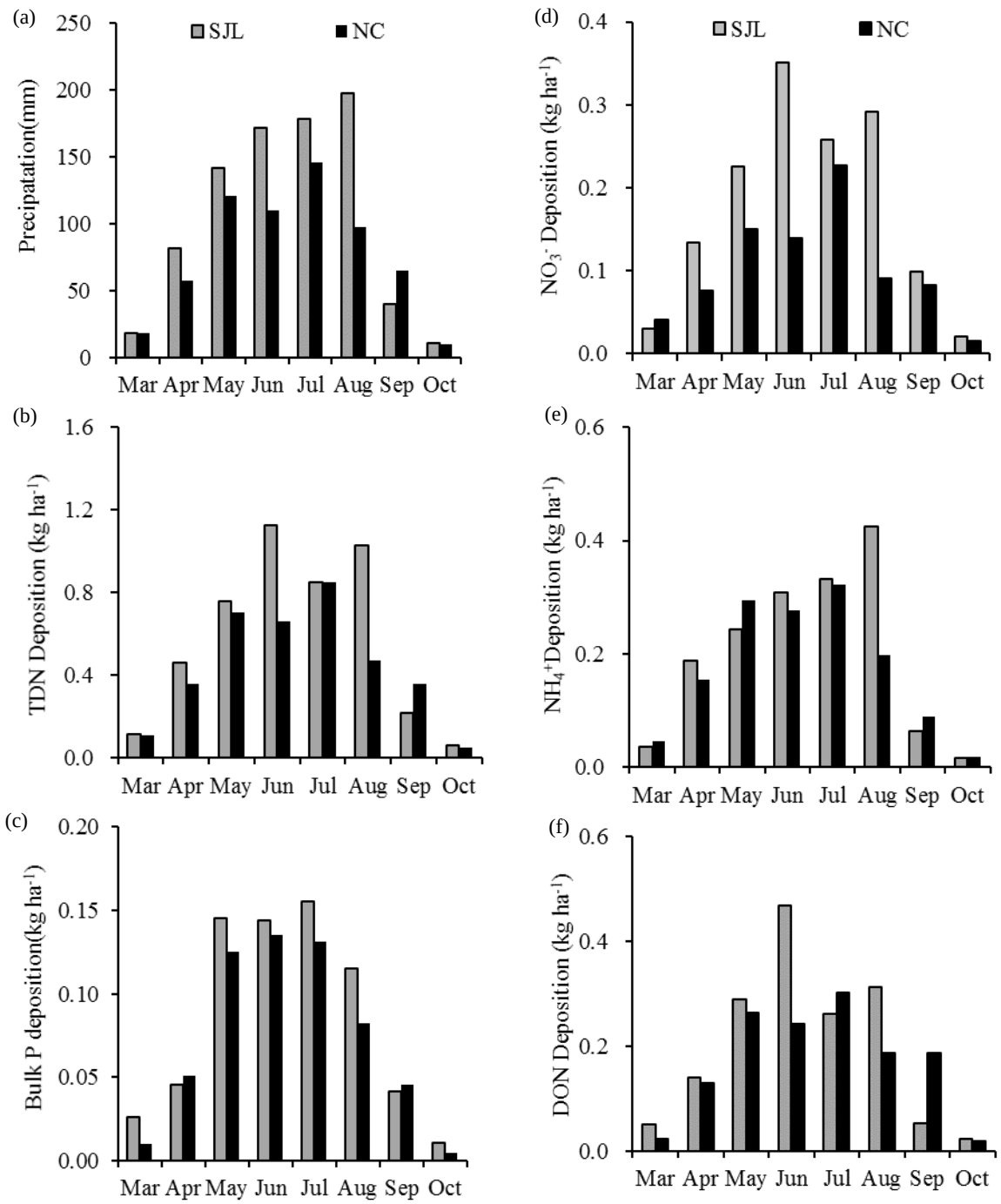

653

654 **Figure 3**

655

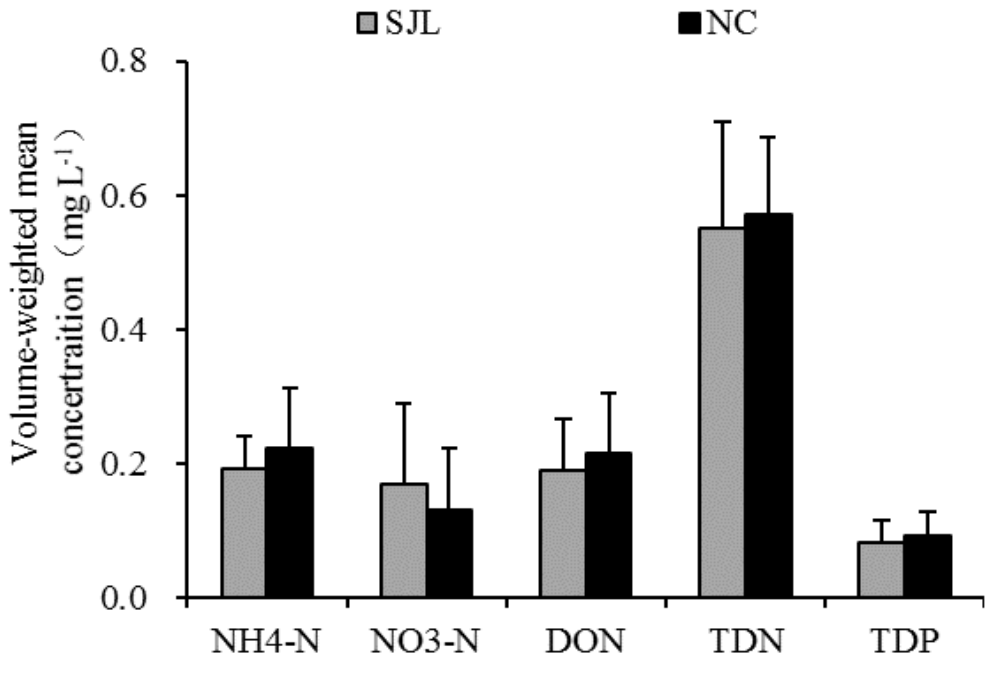


656

657

658 **Figure 4**

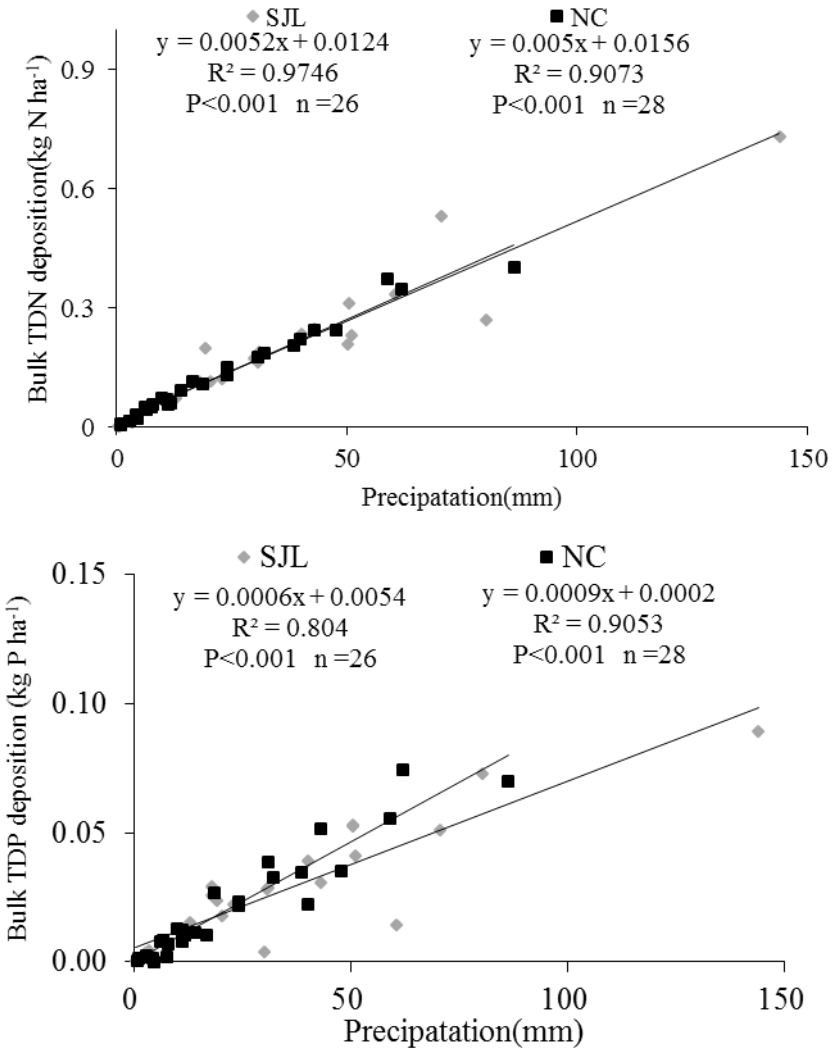


659

660

661 **Figure 5**

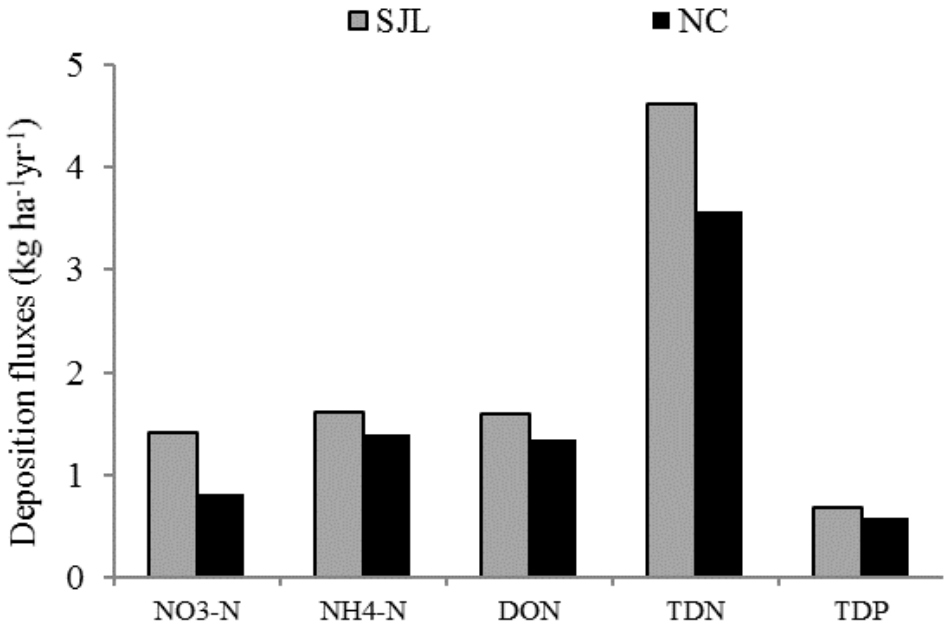


662

663

664 **Figure 6**

665

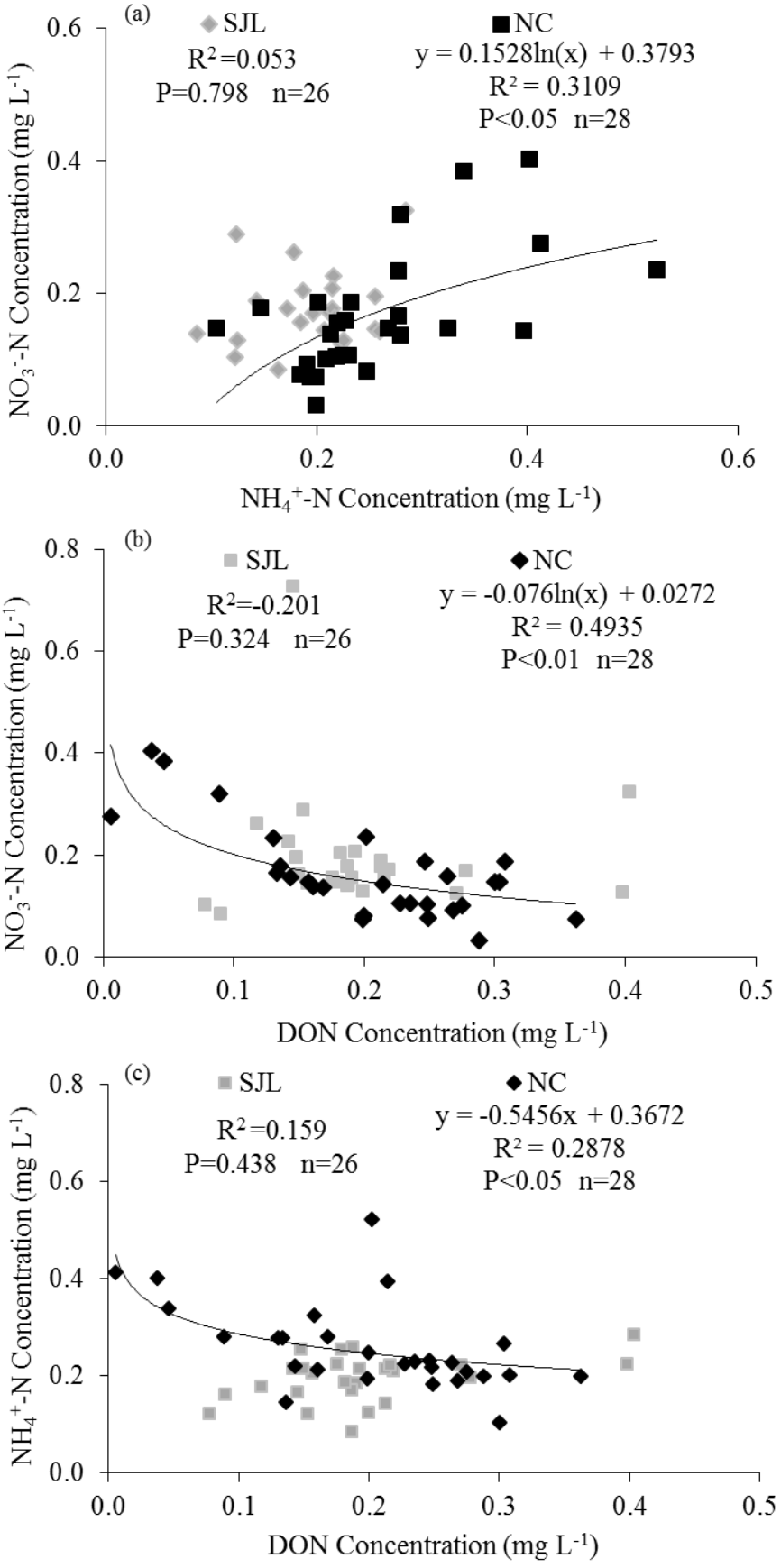

**Figure 7**

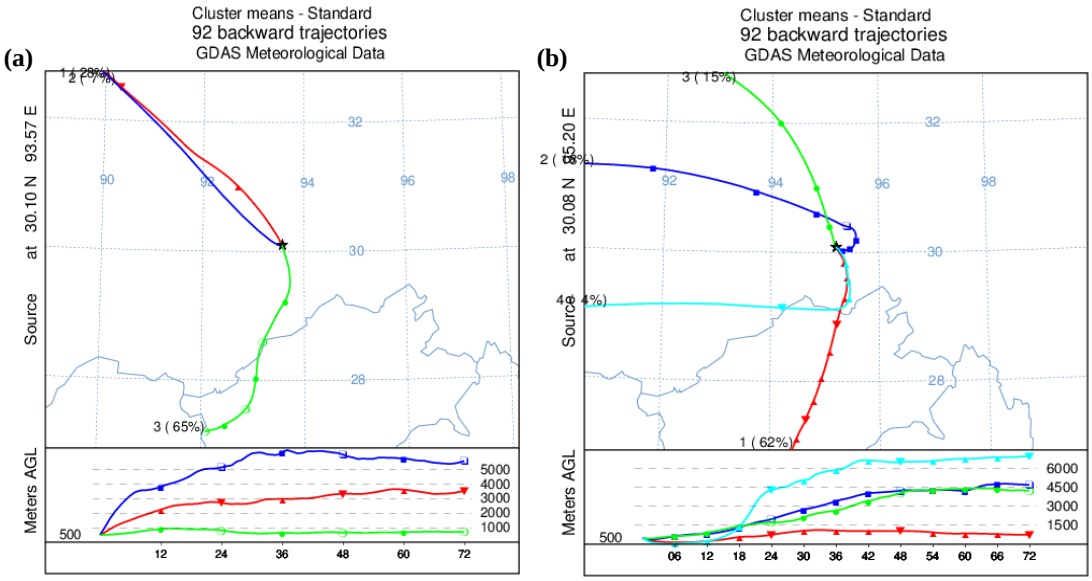
(a)
Cluster means - Standard
92 backward trajectories
GDAS Meteorological Data
Source at 30.10 N 93.57 E
3 ( 65%)
Meters AGL
5000
4000
3000
2000
1000
500
12
24
36
48
60
72
(b)
Cluster means - Standard
92 backward trajectories
GDAS Meteorological Data
Source at 30.08 N 95.20 E
3 ( 15%)
1 ( 62%)
Meters AGL
6000
4500
3000
1500
500
06
12
18
24
30
36
42
48
54
60
66
72

696

**Table 1. Volume weight mean concentration (mg $L^{-1}$) in precipitation under the influences of two categories air masses**

| Site | Direction [a] | $NO_3^-$-N | $NH_4^+$-N | DON | TDN | TDP |
|---|---|---|---|---|---|---|
| NC | S | 0.111 | 0.210 | 0.238 | 0.559 | 0.095 |
| | NW | 0.144 | 0.265 | 0.199 | 0.609 | 0.089 |
| SJL | S | 0.181 | 0.187 | 0.202 | 0.569 | 0.078 |
| | NW | 0.147 | 0.202 | 0.170 | 0.518 | 0.088 |

[a] S: south; NW: northwest.

697